

OMB Number 345-0058

NATIONAL SCIENCE FOUNDATION
1800 G STREET, NW
WASHINGTON, DC 20550

BULK RATE
POSTAGE & FEES PAID
National Science Foundation
Permit No. G-69

PI/PD Name and Address

Dr. William L. Chameides
School of Earth and Atmospheric Sciences
Georgia Institute of Technology
Atlanta, Georgia 30332-0340

NATIONAL SCIENCE FOUNDATION FINAL PROJECT REPORT

PART I - PROJECT IDENTIFICATION INFORMATION

1. Program Official/Org.	Jarvis Moyers
2. Program Name	ATMOS CHEM - (ATM)
3. Award Dates (MM/YY)	From: 880115 To: 910930
4. Institution and Address	School of Earth and Atmospheric Sciences Georgia Institute of Technology Atlanta, Georgia 30332-0340
5. Award Number	ATM 8701289
6. Project Title	Development & Validation of 3-Dimensional Chemical Transport Model

This Packet Contains
NSF Form 98A
And 1 Return Envelope

NSF Grant Conditions (Article 17, GC-1, and Article 9, FDP-II) require submission of a Final Project Report (NSF Form 98A) to the NSF program officer no later than 90 days after the expiration of the award. Final Project Reports for expired awards must be received before new awards can be made (NSF Grants Policy Manual Section 677).

Below, or on a separate page, provide a summary of the completed projects and technical information and attach it to this form. Be sure to include your name and award number on each separate page. See below for more instructions.

PART II - SUMMARY OF COMPLETED PROJECT (for public use)

The summary (about 200 words) must be self-contained and intelligible to a scientifically literate reader. Without restating the project title, it should begin with a topic sentence stating the project's major thesis. The summary should include, if pertinent to the project being described, the following items:

- The primary objectives and scope of the project
- The techniques or approaches used only to the degree necessary for comprehension
- The findings and implications stated as concisely and informatively as possible

SEE ATTACHED

PART III - TECHNICAL INFORMATION (for program management use)

List references to publications resulting from this award and briefly describe primary data, samples, physical collections, inventions, software, etc. created or gathered in the course of the research and, if appropriate, how they are being made available to the research community.

SEE ATTACHED

	7/11/91
Principal Investigator/Project Director Signature	Date

**IMPORTANT:
MAILING INSTRUCTIONS**
Return this *entire* packet plus all attachments in the envelope attached to the back of this form. Please copy the information from Part I, Block I to the *Attention line* on the envelope.

PART II. SUMMARY OF COMPLETED RESEARCH

The three-year subject grant supported a collaborative effort between the Georgia Institute of Technology and NOAA's Geophysical Fluid Dynamics Laboratory aimed at the continued development of a 3-dimensional Chemical Transport Model of tropospheric chemistry. The major focus of these studies was on the elucidation of the global cycle of reactive nitrogen or NO_y compounds. Emissions of nitrogen oxides from fossil fuel combustion and biomass burning, as well as the downward transport of stratospherically-produced nitrogen oxides were found to be inadequate to completely explain the observed concentrations of total NO_y in remote locations of the lower, mid-, and upper troposphere. Thus, it appears that substantial contributions from other sources (such as lightning) are needed to explain the observed NO_y concentrations. Calculations also imply a potentially significant role for PAN-formation in enhancing the long-range transport of NO_y .

PART III. TECHNICAL INFORMATION

The Development and Validation of a
3-Dimensional Chemical Transport Model

FINAL REPORT

W.L. Chameides, P.I.

P. Kasibhatla

School of Earth and Atmospheric Sciences

Georgia Institute of Technology

Atlanta, GA 30332

H. Levy, II, Co-P.I.

Geophysical Fluid Dynamics Laboratory

Princeton, N.J. 08542

This report summarizes our research activities supported by the three-year subject grant. These activities represented a collaborative effort between the Georgia Institute of Technology (GIT) and the NOAA Geophysical Fluid Dynamics Laboratory (GFDL) at Princeton University. The three investigators primarily involved in the study were: Dr. Prasad Kasibhatla, a Research Scientist at Georgia Tech who resides in Princeton and was explicitly hired to implement the joint GIT/GFDL research project, Dr. H. Levy, a GFDL scientist who served as Co-Principal Investigator on the subject grant, and Dr. W.L. Chameides, of Georgia Tech who served as the Principal Investigator on the subject grant. Funds from the subject grant were used principally to support Dr. Kasibhatla's salary and travel expenses related to the collaborative effort. In the sections below we briefly summarize our research results and future plans, and list papers presented and publications that resulted from the subject grant.

I. RESEARCH RESULTS

The overall thrust of the research project has been the development and application of a 3-dimensional Chemical Transport Model (CTM) to study the chemistry of the global troposphere. The long-term goal of this research being to: 1. Elucidate the factors controlling the oxidizing capacity of the atmosphere; 2. Isolate and quantify the influence of human activities on the chemistry of the troposphere; and 3. Contribute to the development of sophisticated coupled chemical/dynamical models of the atmosphere that can serve as predictive tools to study and manage global change.

Main Focus on NO_y: The major focus of our modelling efforts over the three-year grant period has been on quantifying the magnitude and the spatial and temporal variations in the sources and concentrations of reactive nitrogen compounds in the troposphere. Our choice of reactive nitrogen and its sources was based on the mounting theoretical and experimental evidence that the production of tropospheric ozone is largely controlled by the ambient concentrations of nitrogen oxides and the fact that large uncertainties remain in our understanding of the processes that control the global distribution of these compounds, owing to the sparsity of observations.

Our initial study of reactive nitrogen made use of a 3-dimensional, global CTM developed at GFDL. The CTM was used to carry out a series of numerical experiments designed to quantify the distribution of total reactive nitrogen (NO_y) that results from specific NO_x sources; these sources were fossil-fuel combustion, stratospheric photochemical production from N₂O degradation, and biomass burning. In these initial simulations, all NO_y compounds were lumped together as a single species and simple parameterizations were developed to simulate the removal of NO_y via rainout, washout, and dry deposition of specific members of the NO_y family. Comparisons of the

NO_y distributions obtained from these simulations with appropriate observations revealed interesting insights into the relative roles of the NO_x sources in contributing to NO_y in various regions of the globe as well as the possible roles of other sources that are inherently more difficult to simulate (i.e., lightning and soil emissions). The results of this initial study were reported at the International Conference on Global and Regional Atmospheric Chemistry, the Chapman Conference on Global Biomass Burning, and the 7th International Symposium on Atmospheric Chemistry and Global Pollution (see Section III).

Following this initial study, a series of simulations were undertaken with a more sophisticated chemical algorithm that explicitly partitioned NO_y into its major component species. To this end, an off-line chemical scheme was developed to calculate, as a function of latitude, longitude, altitude, time of day, and day of the year, the relative rates at which NO_x , HNO_3 , and PAN are produced and destroyed for a given level of NO_y . These three species were chosen to serve as surrogates for the inorganic insoluble, inorganic soluble, and organic portions of the reactive nitrogen reservoir, respectively. The resulting diurnally-averaged chemical production and destruction rates were incorporated into the model along with more sophisticated wet and dry removal parameterizations. The accuracy of this new scheme was evaluated by running the model with the fossil-fuel-combustion NO_x source and testing its ability to reproduce measured nitrate deposition rates over the eastern United States and Canada. The test revealed encouraging agreement between observations and model-calculations in terms of both temporal and spatial trends.

Thus far the new model has been used to study the impact of downward transport of stratospheric NO_y on tropospheric NO_y concentrations. A detailed description of the results of this study are presented in Kasibhatla et al. (JGR, in press, 1991 and included in Appendix I). Only a couple of salient points are mentioned here. It was found that the stratospheric source was too

small to account for more than a few percent of the observed surface NO_y in the remote lower troposphere. Even in the mid- and upper troposphere, substantial contributions from other sources (such as lightning) are needed to explain the observed NO_y concentrations. It was also found that PAN formation from stratospheric- NO_x can significantly enhance the ability of the atmosphere to transport NO_y from the upper troposphere to the lower troposphere; as a result, neglecting PAN in the stratospheric source calculations has the effect of underestimating surface NO_y mixing ratios in the Northern Hemisphere by factors of 1.5 to 4.

C-Cycle Studies: Another aspect of our research activities has focussed on elucidating the various components of the global C-cycle and more specifically on the nature, magnitude, and distribution of the sources and sinks of atmospheric CO_2 . This work has involved performing CFC-11 transport simulations to test the model's ability to simulate interhemispheric transport as well as initial simulations of atmospheric CO_2 . These initial simulations have corroborated the findings of Tans et al. (1990) that the observed CO_2 latitudinal gradient is incompatible with there being a large CO_2 sink in the Southern Hemisphere Oceans.

II. PLANNED RESEARCH ACTIVITIES

The collaboration between GIT and GFDL initiated by the subject grant remains on-going and is currently being supported through NSF Grant ATM-8905901 to GIT; this grant has approximately one more year till termination. During this next year we plan to complete the model studies of NO_y by carrying out simulations of reactive nitrogen from fossil-fuel combustion, lightning, biomass burning, and soil emissions. In simulations of fossil-fuel combustion and biomass burning, we plan to examine the role of elevated anthropogenic and natural hydrocarbons in causing

enhanced formation of organic nitrates, which may result in enhanced long-range transport of reactive nitrogen from source regions to the remote troposphere. We also plan to carry out studies to help clarify the processes responsible for specific observed phenomena. Examples of these include a study of NO_y transport from industrialized centers to the high northern latitudes, and from African centers of biomass burning to South America.

Our studies of the global C-cycle will also continue. Various source/sink scenarios will be evaluated in terms of their ability to reproduce the observed latitudinal gradients and seasonal patterns of atmospheric CO_2 . We will also examine the feasibility of coupling our atmospheric transport model to one of GFDL's ocean general circulation models.

III. Publications and Presentations:

Thus far two papers have been accepted for publication:

Kasibhatla, P.S., H. Levy, II, W.J. Moxim, and W.L. Chameides, The relative roles of stratospheric photochemical production on tropospheric NO_y levels: A model study, *J. Geophys. Res.*, in press, 1990. (A preprint of this paper is included as Appendix I).

H. Levy II, W.J. Moxim, P.S. Kasibhatla, and J.A. Logan, The global impact of biomass burning on tropospheric reactive nitrogen, in Global Biomass Burning: Atmospheric, Climatic, and Biospheric Implications, ed. by J.S. Levine, MIT Press, Cambridge, Massachusetts, 1991.

In addition the following papers have been presented at meetings:

Global transport from regional sources, International Conference on Global and Regional

Simulated distribution and deposition of reactive nitrogen emitted by biomass burning, Chapman Conference on Global Biomass Burning: Atmospheric, Climatic, and Biospheric Implications, March 19-23, 1990, Williamsburg, Virginia.

Impact of biomass burning on reactive nitrogen levels in the tropics and sub-tropics, 7th International Symposium of the Commission on Atmospheric Chemistry and Global Pollution, September 5-11, 1990, Chamrousse, France.

The global distribution of reactive nitrogen: A synthesis of observation and numerical simulation, 7th International Symposium of the Commission on Atmospheric Chemistry and Global Pollution, September 5-11, 1990, Chamrousse, France.

PART IV — FINAL PROJECT REPORT — SUMMARY DATA ON PROJECT PERSONNEL

(To be submitted to cognizant Program Officer upon completion of project)

The data requested below are important for the development of a statistical profile on the personnel supported by Federal grants. The information on this part is solicited in response to Public Law 99-383 and 42 USC 1885C. All information provided will be treated as confidential and will be safeguarded in accordance with the provisions of the Privacy Act of 1974. You should submit a single copy of this part with each final project report. However, submission of the requested information is not mandatory and is not a precondition of future award(s). Check the "Decline to Provide Information" box below if you do not wish to provide the information.

Please enter the numbers of individuals supported under this grant.
Do not enter information for individuals working less than 40 hours in any calendar year.

	Senior Staff		Post-Doctorals		Graduate Students		Under-Graduates		Other Participants ¹	
	Male	Fem.	Male	Fem.	Male	Fem.	Male	Fem.	Male	Fem.
A. Total, U.S. Citizens										
B. Total, Permanent Residents										
U.S. Citizens or Permanent Residents ² :										
American Indian or Alaskan Native										
Asian										
Black, Not of Hispanic Origin										
Hispanic										
Pacific Islander										
White, Not of Hispanic Origin										
C. Total, Other Non-U.S. Citizens										
Specify Country										
1. INDIA	X									
2.										
3.										
D. Total, All participants (A + B + C)										
Disabled³										

Decline to Provide Information: Check box if you do not wish to provide this information (you are still required to return this page along with Parts I-III).

¹Category includes, for example, college and precollege teachers, conference and workshop participants.

²Use the category that best describes the ethnic/racial status for all U.S. Citizens and Non-citizens with Permanent Residency. (If more than one category applies, use the one category that most closely reflects the person's recognition in the community.)

³A person having a physical or mental impairment that substantially limits one or more major life activities; who has a record of such impairment; or who is regarded as having such impairment. (Disabled individuals also should be counted under the appropriate ethnic/racial group unless they are classified as "Other Non-U.S. Citizens.")

AMERICAN INDIAN OR ALASKAN NATIVE: A person having origins in any of the original peoples of North America, and who maintain cultural identification through tribal affiliation or community recognition.

ASIAN: A person having origins in any of the original peoples of East Asia, Southeast Asia and the Indian subcontinent. This area includes, for example, China, India, Indonesia, Japan, Korea and Vietnam.

BLACK, NOT OF HISPANIC ORIGIN: A person having origins in any of the black racial groups of Africa.

HISPANIC: A person of Mexican, Puerto Rican, Cuban, Central or South American or other Spanish culture or origin, regardless of race.

PACIFIC ISLANDER: A person having origins in any of the original peoples of Hawaii; the U.S. Pacific Territories of Guam, American Samoa, or the Northern Marianas; the U.S. Trust Territory of Palau; the islands of Micronesia or Melanesia; or the Philippines.

WHITE, NOT OF HISPANIC ORIGIN: A person having origins in any of the original peoples of Europe, North Africa, or the Middle East.

THIS PART WILL BE PHYSICALLY SEPARATED FROM THE FINAL PROJECT REPORT AND USED AS A COMPUTER SOURCE DOCUMENT. DO NOT DUPLICATE IT ON THE REVERSE OF ANY OTHER PART OF THE FINAL REPORT.

THE RELATIVE IMPACT OF STRATOSPHERIC PHOTOCHEMICAL PRODUCTION ON TROPOSPHERIC NO_y LEVELS: A MODEL STUDY

P. S. Kasibhatla^{1,2}, H. Levy II³, W. J. Moxim³, and W. L. Chameides¹

Accepted for publication in

J. Geophys. Res.

-
1. School of Earth and Atmospheric Sciences, Georgia Institute of Technology, Atlanta, GA 30332
 2. Currently Visiting Scientist at Geophysical Fluid Dynamics Laboratory, Box 308, Princeton University, Princeton, NJ 08542
 3. Geophysical Fluid Dynamics Laboratory, Box 308, Princeton University, Princeton, NJ 08542

ABSTRACT

The 11-level GFDL global chemical transport model has been used to assess the impact of stratospheric NO_x production on tropospheric reactive nitrogen (NO_y) concentrations. A temporally varying source function was constructed using specified two-dimensional, monthly-average O_3 , N_2O , temperature and surface pressure data generated by the GFDL 'SKYHI' model. The calculated yearly NO_y production rate is 0.64 tg N (0.64×10^{12} g N). A wet removal scheme, which distinguishes between stable and convective rain based on the bulk Richardson number, is introduced. Simulations have been performed with a simplified chemical mechanism which fractionates NO_y into soluble and insoluble species. The role of PAN in determining the impact of stratospheric injection on the tropospheric NO_y budget is studied by comparing results of simulations with and without PAN chemistry. We conclude that: (1) The stratospheric source is too small to account for background surface NO_y concentrations observed in the remote (i.e., regions a few thousand kilometers from continental source regions) troposphere. Surface NO_y mixing ratios seldom exceed 10 pptv in the model Northern Hemisphere, and are always below 20 pptv. Together, fossil-fuel combustion emissions and stratospheric injection account for less than 10% of observed surface nitrate concentrations in the remote tropical Pacific; (2) The impact of the stratospheric source is comparable to that of the fossil-fuel combustion source in terms of NO_y mixing ratios in the Northern Hemisphere at the 500 mb model level, and is more important in the mid- and high latitudes of the Southern Hemisphere. At the 315 mb model level, the stratospheric source contribution to NO_y levels is more important than that of the fossil fuel source at all latitudes, except in the tropics. However, substantial contributions from other NO_y sources are needed to explain observations in the remote mid- and upper troposphere; and (3) Inclusion of PAN chemistry has the effect of increasing model-calculated surface NO_y mixing ratios in the Northern Hemisphere mid- and high latitudes by factors of 1.5-3 during winter/spring, and by factors of 2-4 during summer/fall. Surface NO_y mixing ratios in the Southern Hemisphere show a smaller

increase due to slower rates of PAN formation. This is a direct result of lower hydrocarbon concentrations in the Southern Hemisphere.

1. INTRODUCTION

The importance of reactive nitrogen compounds (NO_y) in atmospheric chemistry over a variety of spatial and temporal scales has long been recognized. Nitrogen oxides ($\text{NO}_x = \text{NO} + \text{NO}_2$) play a major role in determining the global oxidizing power of the troposphere by controlling tropospheric O_3 (Crutzen, 1974) and OH levels (Levy, 1971). Thus, they may have a significant influence on global climate through their indirect impact on the rate of removal of greenhouse gases from the atmosphere. NO_x has also been shown to be an important precursor to urban photochemical smog formation (Leighton, 1961), and HNO_3 is one of the two important acidic components of acid rain (National Research Council, 1983). In addition, nitrate is an important nutrient to oceanic ecosystems (Ryther and Dunstan, 1971).

A comprehensive knowledge of the key factors affecting NO_y distributions is essential if one attempts to isolate the influence of humans on atmospheric chemistry in particular, and on global climate in general. Our present understanding of the factors controlling the distribution of NO_y is extremely limited due to the sparsity of available observational data, especially in remote regions of the world. In this context, models provide us with a valuable tool to synthesize the knowledge gained from limited field studies, and to extrapolate the data to more representative global scenarios.

A fundamental question, that remains largely unanswered, relates to the nature, magnitude, and spatial and temporal variation of the various sources of NO_y . Levy and Moxim (1989) simulated the global distribution and deposition of NO_y emitted by fossil-fuel combustion. These emissions are mainly concentrated in the northern mid-latitudes, with a global annual source strength of approximately 21 Tg N (21×10^{12} g N). Their analysis showed that while these emissions were sufficient to account for a large fraction of observed surface NO_y levels near source regions in the Northern Hemisphere, they were insufficient to account for more than ~10% of observed background levels in the remote tropics and in the Southern Hemisphere. They speculated that other possible sources of

NO_x such as biomass burning, production by lightning, biogenic emissions, and stratospheric injection may make important contributions to the tropospheric NO_y budget. With the exception of the stratospheric source, these sources are inherently difficult to quantify owing to their nature, and due to their geographical distribution.

Based on a simulation with an idealized source, Levy *et al.* (1980) hypothesized that the stratospheric source could account for at least half the NO_y present in the remote tropics and in the Southern Hemisphere. Liu *et al.* (1980) carried this one step further, arguing that downward transport of NO_x produced in the stratosphere, and subsequent photochemical production of O_3 in the upper troposphere, could be a significant source of tropospheric O_3 . Their calculations used the NO_y fields predicted by Levy *et al.* (1980), along with semi-empirically derived NO_x/NO_y ratios from Kley *et al.* (1981). On the other hand, Logan (1983) argued that the stratospheric flux was too small to have a significant impact on tropospheric NO_y levels, and suggested that Levy *et al.* (1980) had used unrealistically long rainout lifetimes in their model calculations. Recent analysis of surface observations in the tropical Pacific also suggests that the stratospheric source may have a minimal impact on surface NO_y concentrations (Savoie *et al.*, 1989).

In the above mentioned model studies, Levy *et al.* (1980) and Levy and Moxim (1989) treated the collection of reactive nitrogen compounds as a single species, namely NO_y . By using effective dry and wet removal coefficients for NO_y , an attempt was made to implicitly capture the effect of chemical transformations and removal of individual species on the distribution and deposition of total reactive nitrogen. A problem arises, however, in arriving at *a priori* estimates of wet and dry removal coefficients for an arbitrary source distribution. Even for a particular source function, such as the fossil fuel combustion source, where observed deposition fluxes provide a constraint against which model parameters may be adjusted over source regions, it is by no means certain that removal rates will be calculated 'correctly' in regions remote from the source region. The approach taken in this paper is therefore a more fundamental one. We explicitly treat NO_x , HNO_3 , and PAN as

transported species, using a simplified chemical scheme to calculate chemical production and destruction rates for each of these species.

This study focuses on a reexamination of the potential impact of stratospheric photochemical NO_x production on tropospheric NO_y levels. We therefore present an analysis of the results of a set of model simulations with this stratospheric source alone. An assessment of the relative impact of this small source ($0.64 \text{ tg N year}^{-1}$) is provided by comparing model results with available observations of tropospheric NO_y mixing ratios and deposition fluxes. Similar studies with other individual sources are presently underway, and will be discussed in future papers.

2. BRIEF DESCRIPTION OF THE MODEL

The global chemical transport model (GCTM) has a horizontal resolution of ~ 265 km, and 11 vertical levels at standard pressures of 990, 940, 835, 685, 500, 315, 190, 110, 65, 38, and 10 mb. The model is driven by 6-hour time-averaged wind and total precipitation fields derived from a one year integration of a parent general circulation model (GCM) (Manabe *et al.*, 1974; Manabe and Holloway, 1975). The meteorological features of the GCM have been the subject of many previous studies, and the interested reader may wish to refer to the paper by Mahlman and Moxim (1978) for a comprehensive list of references pertaining to the GCM, and an encapsulated review of the GCM climatology pertinent to this study. However, a few remarks on the dynamics of stratosphere-troposphere exchange processes in the model are appropriate here. The meridional circulation in the GCM consists of a 3-cell troposphere, a 2-cell Northern Hemisphere stratosphere, and a 3-cell Southern Hemisphere stratosphere, with midstratospheric flow from the summer to winter hemisphere. A detailed description of the simulated dynamics in the stratosphere is given by Manabe and Mahlman (1976). The tropopause appears at the proper altitudes, and its poleward downward slope agrees well with observations. Mahlman and Moxim (1978) found in their midlatitude instantaneous source experiment that the global mean

vertical transport across the tropopause is dominated by eddy transport. At particular latitudes, however, the eddy transport is of the same order of magnitude as the mean transport, reflecting the fact that eddy transport is predominantly downward, while the mean transport may be upward or downward. In their study, strongest downward eddy cross-tropopause fluxes occur near 50-60°N during March-May, associated with upper tropospheric cyclogenesis, while strongest downward zonal-mean fluxes occur near 35-45°N during December-February. An analysis of the transport of an ozone-like tracer by Mahlman *et al.* (1980) found that the annually-averaged Northern Hemisphere cross-tropopause flux was approximately 1.8 times larger than the corresponding flux in the model Southern Hemisphere. Their study also suggests that the model may considerably underestimate cross-tropopause tracer fluxes in the Southern Hemisphere.

The GCTM incorporates parameterizations for approximating horizontal sub-grid scale transport, vertical mixing by dry and moist convection, and vertical mixing in the boundary layer under conditions of large scale stability. Dry deposition is calculated based on the assumption of a balance between surface deposition and the turbulent flux in the bottom half of the lowest level in the model. The deposition velocities used in the model (indicated in section 3) reflect measured deposition velocities of individual reactive nitrogen species. A more detailed description of these and other features of the GCTM can be found in studies by Mahlman and Moxim (1978), Levy *et al.* (1982), Levy *et al.* (1985), and Levy and Moxim (1989). A significant change in the present application of the model is the manner in which wet removal rates are calculated. Our current scheme, the main ideas of which are borrowed from Giorgi and Chameides (1986), is outlined in more detail below.

Consider a column of grid boxes in which precipitation occurs. Let A_B and H represent the cross-sectional area and height of the column, respectively, and F represent the fraction of the cross-sectional area over which precipitation occurs. We now assume that for a highly soluble tracer (such as HNO_3) F is also the fraction of the tracer originally present in a box that is removed during a precipitation event. Wet deposition rates for a

highly soluble tracer, at each time step and each grid box, can then be calculated as

$$\left. \frac{\partial R}{\partial t} \right|_{(wet)} = \frac{-FR}{\Delta t}, \quad (2.1)$$

where, R is the tracer mixing ratio. We now have to determine F . If L is the liquid water content of the 'cloud', and Q is the precipitation rate averaged over the column cross-sectional area, the volume of 'cloud', V_c , is

$$V_c = \frac{A_B Q \Delta t \rho}{L}, \quad (2.2)$$

where, ρ is the density of liquid water. We use the term 'cloud' in the same sense as Giorgi and Chameides (1986), i.e., to refer to that fraction of the grid where precipitation is occurring. The fraction of the column cross-sectional area over which precipitation, and therefore wet removal, occurs is then

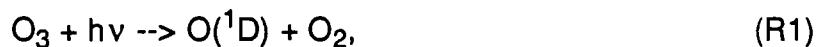
$$F = \frac{V_c}{HA_B} = \frac{Q \Delta t \rho}{LH}. \quad (2.3)$$

Equations 2.1 and 2.3 together represent the parameterization for wet removal, based on GCM-derived precipitation intensity fields, that is used in the GCTM for a highly soluble species. In the actual application of the scheme, the height H is specified to be the height of the top of the 685 mb layer in the model except when there is convective instability as determined by the moist Richardson number (Ri_m) calculated at the 500 mb and 315 mb levels. The mathematical expression used to calculate Ri_m is given by Levy *et al.* (1982). If Ri_m is less than 0.25 for the 315 mb level, wet removal is assumed to occur from the ground to the top of the 315 mb layer. Similarly, if Ri_m is greater than 0.25 for the 315 mb level, but less than 0.25 for the 500 mb level, wet removal is assumed to occur from the ground to the top of the 500 mb layer. We use the term 'convective rain' to characterize precipitation events for which Ri_m is less than 0.25 at the 315 or 500 mb model levels. All other precipitation events are termed 'non-convective'. Values for L are the same as those used by Giorgi and Chameides (1986), with $L = 2 \times 10^{-6} \text{ g cm}^{-3}$ for convective rain, and L

= $0.5 \times 10^{-6} \text{ g cm}^{-3}$ for non-convective rain. We have performed some preliminary tests with this scheme by simulating the global distribution of NO_y resulting from fossil-fuel combustion emissions only. These simulations indicate that model-calculated wet deposition fluxes agree with observed wet deposition fluxes in North America and Europe (where fossil-fuel combustion emissions dominate the NO_y budget) at least as well as previous calculations by Levy and Moxim (1989) in which a different wet removal scheme was used. In addition, nitrate wet deposition fluxes at sites in the North Atlantic which are mainly impacted by fossil-fuel combustion are well simulated.

3. DESIGN OF THE EXPERIMENTS

NO is produced in the stratosphere by the following reaction sequence:



Reaction R1 generates highly reactive atomic oxygen, which is either quenched by collision with molecular oxygen and nitrogen (reaction R2), or reacts with nitrous oxide (transported to the stratosphere from the troposphere) to yield two molecules of NO per atom of oxygen reacting with N_2O (reaction R3). Using monthly- and zonally-averaged O_3 and N_2O fields (shown in Figure 1 for the months of January and July), along with corresponding temperature and surface pressure data from the GFDL 'SKYHI' GCM which has a higher vertical resolution (Hamilton and Mahlman, 1988), we have calculated diurnally averaged NO production rates for the middle of each month based on reactions R1-R3. Kinetic data used in the calculations were obtained from DeMore *et al.* (1990). The calculated NO production rates for four months representing winter, spring, fall, and summer are shown in Figure 2. The seasonal variation of the NO production rate is clearly seen, with maximum production occurring in the summer hemisphere. Maximum production

rates ($\sim 200 - 240 \text{ molecules cm}^{-3} \text{ s}^{-1}$) occur near the equator at approximately 10 mb. The calculated annual NO production rate is 0.64 tg N. This estimate is consistent with recent estimates of 0.4-0.7 tg N/year (Crutzen and Schmailzl, 1983), and 0.7 tg N/year (Legrand *et al.*, 1989). Jackman *et al.* (1980) have argued that the production of NO by galactic cosmic rays in the lower stratosphere and upper troposphere is comparable to the production of NO by N_2O oxidation at latitudes poleward of $\sim 50^\circ$. On a global scale, however, N_2O oxidation is the dominant stratospheric NO_x source. As we shall see later, our conclusions regarding the tropospheric impact of the stratospheric source are mainly drawn by comparing model results with measurements in the remote tropics and sub-tropics. Our conclusions, therefore, are not significantly affected by the fact that we have considered only the photochemical NO_x source in the present study. In addition, NO_x emitted in the exhaust fumes of jet aircraft may contribute locally to NO_y levels in midlatitudes, but we have made no attempt to quantify the effect of this source. Calculated source strengths were gridded to the GCTM grid, and specified in the form of a 'look-up' table in the model. We should point out that although the top model full-level is at 10 mb, the top model layer extends from ~ 27 mb to the top of the atmosphere. Daily NO production rates were calculated in the GCTM by time-interpolating between appropriate table values.

The chemical partitioning of NO_y into soluble and insoluble fractions was calculated using a simple chemical scheme, and using NO_x and HNO_3 as surrogates for insoluble and soluble reactive nitrogen species, respectively. Details of the chemical scheme are given in the appendix. Deposition velocities for HNO_3 (1.0 cm s^{-1} over land; 0.5 cm s^{-1} over ocean) and for NO_x (0.2 cm s^{-1} over land; 0.0 cm s^{-1} over ocean) were selected based on the annual average of available measurements over land (Cadle *et al.*, 1985; Huebert and Robert, 1985; Wesely *et al.*, 1982; Walcek *et al.*, 1986; Voldner *et al.*, 1986). Calculation of wet deposition involves treating NO_x as an insoluble species, and using equations 2.1 and 2.3 to determine HNO_3 removal rates. We treat this simulation as our base case simulation, and will hereafter refer to it as the CASE1 experiment.

We next focus on the role of long-lived, reservoir organic species formation in determining tropospheric NO_y concentrations. The chemistry involved in the formation and destruction of these organic constituents is extremely complex (Madronich and Calvert, 1990). In addition, many of the reaction rates and products are not well characterized. In this study, we therefore attempt to provide only a zeroth order analysis of the impact of such a sequestration on the tropospheric NO_y burden. We use peroxyacetyl nitrate (PAN) as a surrogate for the organic NO_y species, and calculate PAN production and destruction rates using a specified hydrocarbon distribution. PAN production is assumed to occur only at or below the 190 mb model level equatorward of 45° latitude, and at or below the 315 mb model level poleward of 45° latitude. Our scheme considers six reactions:



where, HC and PAC refer to hydrocarbons and peroxyacetyl radical, respectively.

By assuming that PAC is in photochemical equilibrium, the production rate of PAN is given by

$$P_{\text{PAN}}^S = k_{P2} \left[\frac{k_{P1} n(\text{HC}) n(\text{OH})}{k_{P2} n(\text{NO}_2) + k_{P3} n(\text{NO}) + k_{P4} n(\text{HO}_2)} \right] \frac{n(\text{NO}_2)}{n(\text{NO}_X)} n(\text{NO}_X^S), \quad (3.1)$$

where, the n 's represent number densities, and k_j is the specific reaction rate for reaction j . Number densities of OH, HO₂, NO, NO₂, and NO_x are calculated using the scheme described in the appendix, and the superscript 's' refers to quantities derived in the transport model from the stratospheric source alone. Similarly, the PAN destruction rate is

$$\tau_{PAN^S} = \left[k_{P6} n(OH) + \frac{k_{P5} \{ k_{P3} n(NO) + k_{P4} n(HO_2) \}}{k_{P2} n(NO_2) + k_{P3} n(NO) + k_{P4} n(HO_2)} \right] n(PAN^S). \quad (3.2)$$

In this study we use ethane as a surrogate for all hydrocarbons which produce PAC, and specify uniform ethane mixing ratios of 2 and 0.4 ppbv in the northern and southern hemispheres, respectively, based on measured hydrocarbon concentrations in the background atmosphere (Singh and Zimmerman, 1990; Rudolph, 1988). Kinetic data for reaction P1 is obtained from DeMore *et al.* (1990), while rate constants recommended by Atkinson and Lloyd (1984) are used for reaction P2, P3, and P5. It should be noted that the rate of thermal decomposition of PAN (reaction P5) is highly temperature sensitive ($k_{P5} = 1.95 \times 10^{16} e^{-13543/T} \text{ s}^{-1}$). PAN formation at low temperatures, therefore, provides a pathway by which some of the NO_y can be sequestered in a stable form. Subsequent long-range transport of PAN can then serve as a potentially important source of NO_y in the remote troposphere. There is some uncertainty regarding the products of reaction P6. In this study, we assume reaction P6 to be a chemical source of NO_x , with $k_{P6} = 1.23 \times 10^{-12} e^{-651/T} \text{ cm}^3 \text{ molecules}^{-1} \text{ s}^{-1}$ (Singh *et al.*, 1991a). We further assume that PAN has neither dry nor wet sinks, thus providing an upper limit of the impact of tropospheric PAN production on the global NO_y burden resulting from stratospheric injection. This model experiment will be referred to as CASE2.

The results of our model calculations are presented in the next section. Section 4.1 focuses on the zonal-mean mixing ratio fields from the CASE1 experiment, while the CASE2 simulation is compared with the CASE1 experiment in section 4.2. A more detailed analysis of surface and mid- and upper tropospheric NO_y mixing ratios is presented in section 4.3 and 4.4.

4. RESULTS OF THE EXPERIMENTS

The GCTM CASE1 simulation was initialized with a one-dimensional NO_y profile, varying from ~50 pptv at the surface to ~17.5 ppbv at 10 mb. On the model start-up date

of October 1, this initial NO_y field was partitioned into NO_x and HNO_3 on the basis of chemical production and destruction rates calculated using the simple chemical scheme described in the appendix. The model was integrated for a period of 64 months, at which time globally- and annually-averaged sources and sinks were essentially in balance for both NO_x and HNO_3 . The CASE2 simulation was initialized with NO_x and HNO_3 distributions obtained after integrating the CASE1 simulation for 28 months. In addition, a uniform background mixing ratio of 1 pptv was used to initialize PAN, and the model was integrated for a period of 36 months. In the rest of this paper we will focus on the resulting steady-state distributions, and hence all subsequent discussions will refer to model fields from the last 12 months of each experiment. While this study will be mainly confined to an analysis of the resulting tropospheric mixing ratio fields, and comparisons of these model fields with available observations, we will also examine the zonal-mean distribution of NO_y and its constituents from the mid-stratosphere to the surface.

4.1 Zonal-mean mixing ratio fields from the CASE1 experiment

Monthly-average, zonal-mean NO_y fields from the CASE1 experiment are shown in Figure 3 for the months of January, April, July, and October. The familiar feature of poleward-downward sloping isopleths is seen, with higher mixing ratios occurring poleward and lowest values at or near the equator. Seasonal variations in mid-latitude tropospheric mixing ratios are evident, with maximum values occurring during winter and spring in each hemisphere. Another interesting feature is the steepening of tracer mixing ratio isolines at high northern latitudes during the transition from spring to summer. Mahlman and Moxim (1978) put forward the diagnostic interpretation that this was due to a diminished degree of self-cancellation between mean and eddy effects during the seasonal transition. A similar feature is not evident in the model Southern Hemisphere, and appears to be a model defect.

The stratospheric source appears to be significant relative to the fossil-fuel com-

bustion source in terms of mid- upper tropospheric NO_y mixing ratios in mid-latitudes, especially during winter and spring. At the 500 mb model level, the stratospheric source yields zonal-mean NO_y mixing ratios of approximately 100 pptv in the Northern Hemisphere mid-latitudes. This is comparable to estimates of zonal-mean NO_y resulting from the combustion source alone (Levy and Moxim, 1989). In addition, model NO_y mixing ratios from the stratospheric source (200-500 pptv) are a factor of 2-10 higher than those produced by the combustion source in the northern mid-latitudes at 315 mb. The stratospheric source is also clearly more important than the fossil-fuel combustion emission source in the Southern Hemisphere mid-troposphere as evidenced by the very low NO_y levels (2-10 pptv) calculated by Levy and Moxim (1989) in their fossil-fuel combustion experiment. The results from the CASE1 simulation also seem to indicate that the stratospheric source has only a small impact on surface NO_y where model mixing ratios are generally below 5 pptv, with slightly higher values at high latitudes.

A closer examination of Figure 3 also reveals a significant interhemispheric asymmetry in mid-tropospheric mixing ratios, with higher mixing ratios in the Northern Hemisphere. While the annually-averaged NO_y source has no interhemispheric asymmetry, some asymmetries arise due to differences in wet and dry removal rates in the two hemispheres. However, the major difference between the two hemispheres is the considerably weaker poleward-downward transport from the production region in the middle stratosphere to the lower stratosphere in the model Southern Hemisphere (Mahlman *et al.*, 1980). While this asymmetry is to be expected on the basis of stratospheric dynamics, it may be exaggerated in this model.

Table 1 shows a comparison between LIMS derived NO_y for January 1979 (World Meteorological Organization, 1985) and model simulated NO_y at 50 mb. NO_y mixing ratios in the Northern Hemisphere extratropical stratosphere are reasonably well simulated, though the slight overestimate in the tropics and underestimate in the mid-latitudes indicates that the slopes of the mixing ratio isopleths are too flat. Mahlman *et al.* (1986) ob-

tained a similar result in their simulation of stratospheric N_2O . They found that observed meridional slopes of mixing ratio isolines were steeper than those simulated by the model by about 30%. Their analysis showed that this discrepancy was caused by the fact that the magnitude of meridional gradient of net diabatic heating was underestimated in the model, leading them to conclude that the magnitude of the dynamical drive in the model stratosphere was too weak. The model underestimates NO_y in the high latitude lower stratosphere of the Southern Hemisphere, again suggesting that poleward-downward transport from the middle stratosphere is too weak in the model Southern Hemisphere.

It is also interesting to compare model results from this experiment with those from Mahlman *et al.* (1980) involving an ozone-like tracer. In that study, the latitudinal tracer gradient at the 10 mb model level is maintained by relatively fast photochemistry, with the result that maximum mixing ratios at the top model level occur in the tropics (see Figure 3.3, Mahlman *et al.*, 1980). In sharp contrast, in the present study highest NO_y mixing ratios at 10 mb occur at high latitudes, reflecting the dominant role of transport processes in establishing the latitudinal NO_y gradient at that level. In spite of this striking dissimilarity in tracer distributions at the top model level, slopes of the mixing ratio isopleths in the lower stratosphere are remarkably similar in the two studies. This is due to the fact that in both studies it is the average stratification of tracer between the middle and lower stratosphere that determines the tracer structure in this region (Mahlman *et al.*, 1980).

Zonally-averaged NO_x and HNO_3 distributions for January and July are shown in Figure 4. While HNO_3 mixing ratios are 2-3 times higher than those of NO_x in the extratropical lower stratosphere, NO_x is more abundant above the 38 mb model level in the equatorial stratosphere due to the fact that the local NO_x photochemical source is largest in this region, and also due to the relatively rapid rate of HNO_3 photolysis in this region. In the mid- and upper extratropical troposphere, however, HNO_3 mixing ratios are significantly higher than NO_x levels. For example, HNO_3 mixing ratios range from 50 pptv to greater than 200 pptv, while the corresponding NO_x mixing ratios are 20-100 pptv pole-

ward of 30° N in January at the 315 mb model level. This can be explained on the basis of the fact that the rate of chemical conversion of HNO₃ to NO_x decreases more rapidly in going from the stratosphere to the middle troposphere than does the rate of chemical production of HNO₃ from NO_x. Scavenging of HNO₃ by precipitation becomes important below 315 mb, complemented by the faster rate of dry removal of HNO₃ at the surface, leading to comparable abundances of NO_x and HNO₃ near the surface in the summer hemisphere. NO_x surface mixing ratios in the extratropics exhibit a significant seasonal maximum in winter because OH levels are much lower during this period.

4.2 Comparisons of zonal-average NO_y fields from the CASE1 and CASE2 experiments

The previous section has highlighted the fact that in the model the stratospheric source appears to have only a minimal impact on lower tropospheric NO_y mixing ratios. A large fraction of the NO_y transported down from the stratosphere is in the form of HNO₃. The fraction of NO_y injected into the troposphere in the form of NO_x is converted relatively rapidly to HNO₃, which is removed quite efficiently by wet and dry sinks in the lower troposphere. There has been some speculation that formation of relatively long-lived organic nitrogen species (such as PAN) from NO_x could serve to increase the overall lifetime of NO_y in the troposphere. According to this argument, the organic species serve as temporary reservoirs for active nitrogen. For example, this mechanism, applied to fossil-fuel combustion emissions, has been used in an attempt to explain NO_x and O₃ mixing ratios observed in the high latitude troposphere over North America and Greenland during the ABLE-3A experiment (Singh *et al.*, 1991a; 1991b).

In this section, we focus on the question of whether the sequestering of NO_x into temporary organic reservoirs might affect model calculated tropospheric NO_y mixing ratios, and attempt to assess the magnitude of this effect. We feel that the design of the CASE2 experiment provides a realistic upper limit of the impact of tropospheric production of organic nitrogen species on NO_y distributions resulting from the stratospheric source

(refer to the discussion in section 3).

Figure 5 illustrates the differences in NO_y fields between the CASE2 and CASE1 simulations. Inclusion of PAN chemistry in the model does not alter simulated NO_y levels by more than 10% above 500 mb since the wet sink is relatively weak above this level. The CASE2 simulation yields enhanced NO_y mixing ratios, usually by factors of 1.3-4, in the mid- and high latitude lower troposphere. The magnitude of the effect is generally larger in the northern hemisphere, except during the northern winter. This is a direct consequence of higher PAN production rates in the Northern Hemisphere which is a result of the interhemispheric difference in hydrocarbon concentrations. In spite of the extreme sensitivity of the rate of PAN decomposition to temperature, the model results show the counter-intuitive feature that PAN formation has a smaller effect on lower tropospheric NO_y levels at higher latitudes in winter. This is because photochemical activity (and therefore conversion of NO_x to HNO_3 , as well as PAN formation in the upper troposphere) is greatly suppressed in winter at high latitudes. Inclusion of the PAN reactions also has a relatively minor effect (10-20%) on tropical surface NO_y mixing ratios owing to the rapid rate of thermal decomposition of PAN.

These differences in total NO_y fields between the two experiments can be related to the corresponding changes in NO_x and HNO_3 fields (Figure 6). We will illustrate our discussions with model results from January and July. In the following discussion, we shall use the terms "suppressed" and "enhanced" to refer to changes relative to the CASE1 experiment, i.e., relative to the simulation with no PAN chemistry. Net photochemical production of PAN has the effect of suppressing NO_x mixing ratios in the mid- and upper troposphere. During January, the largest effect on NO_x occurs in a relatively small region centered around 500 mb in the northern tropics, and also in the mid-troposphere of the high latitude Southern Hemisphere. Thermal decomposition of PAN subsequently serves as a source of NO_x (some of which is converted to HNO_3) in the lower troposphere, leading to enhanced levels of NO_x and, to a lesser extent, of HNO_3 near the surface. A similar

picture unfolds in July, though on a larger spatial scale. NO_x mixing ratios are suppressed by at least 10% over most of the Northern Hemisphere between 315 and 500 mb. HNO_3 levels in this region are also suppressed, since some of the NO_x which would otherwise be converted to HNO_3 is now sequestered in the form of PAN. PAN decomposition leads to enhanced NO_x mixing ratios in the lower troposphere, by factors of 2-5, over a broad region extending poleward from 30°N , with corresponding HNO_3 mixing ratios enhanced by 10-50%. Inclusion of PAN chemistry has a greater impact on Northern Hemisphere model results due to the aforementioned interhemispheric difference in hydrocarbon mixing ratios. This fact is also illustrated in model-simulated PAN distributions (see Figure 7). During the southern summer, the highest PAN mixing ratios are of the order of 2-5 pptv. By contrast, model-simulated PAN mixing ratios range from 10-20 pptv in the mid- and upper troposphere of the extratropical Northern Hemisphere during July. The rapid rate of thermal decomposition of PAN results in extremely low PAN mixing ratios in the tropical lower troposphere. This result is consistent with measurements by Rudolph and Muller (1990) in the remote South Atlantic, where surface PAN levels were typically below 0.5 pptv.

Our results therefore suggest that sequestering of active nitrogen into relatively long-lived, temporary reservoirs (such as PAN) could be important, especially in the mid- and higher latitudes of the Northern Hemisphere lower troposphere where neglecting this effect may cause NO_x levels to be underpredicted by factors of 1.5 to > 5 . Such a mechanism could presumably be equally significant for other NO_y sources, and especially for the upper tropospheric lightning source. We caution, however, that these results should be interpreted with some care since the chemistry involved is quite complex and not yet fully understood. The results from the CASE2 experiment should therefore be viewed in the context of providing an upper limit to our calculations of the tropospheric impact of the stratospheric NO_y source, while the CASE1 results provide the corresponding lower limit.

4.3 Surface mixing ratios

One of the main thrusts of this study is to examine the impact of stratospheric production on surface NO_y mixing ratios. As mentioned earlier, a previous study by Levy and Moxim (1989) found that emissions from fossil-fuel combustion could account for less than 10% of observed surface NO_y in regions remote from the predominantly Northern Hemisphere, midlatitude source regions. Based on results scaled from a stratified tracer experiment (Mahlman *et al.*, 1980), Levy *et al.* (1980) hypothesized that stratospheric production of NO could be a significant source of NO_y for the remote troposphere, accounting for up to half the observed NO_y in these regions. Their model calculated, surface mixing ratios were in reasonable agreement with the lowest NO_y concentrations measured over the equatorial Pacific (Huebert, 1980). Levy and Moxim (1989) also used the fact that seasonal cycles of surface O_3 (Oltmans, 1981) and surface aerosol nitrate (Savoie *et al.*, 1989) at Samoa were similar, as an argument in favor of an upper tropospheric or stratospheric source of NO_y in the remote troposphere. However, calculations by Savoie *et al.* (1989) revealed that there was almost no correlation between measured surface ^7Be and aerosol nitrate, and between surface O_3 and aerosol nitrate, and they concluded that the stratosphere has a minimal impact on tropospheric NO_y .

In this section we readdress some of these issues by comparing model simulations of surface NO_y with earlier estimates by Levy *et al.* (1980). The major differences between the two studies are the explicitly calculated NO_y source distribution, the partitioning of NO_y into NO_x , HNO_3 , and PAN (in the CASE2 experiment) in the current study, and in the wet removal parameterization used. We will also present some comparisons of our results with an estimate by Levy and Moxim (1989) of surface NO_y distributions resulting from fossil-fuel combustion emissions alone, in an attempt to identify regions where the small stratospheric source could be of importance. We emphasize, however, that such an evaluation is preliminary since the fossil-fuel combustion experiment by Levy and Moxim (1989) differs in terms of the number of transported species, and the wet removal scheme

used in the model. We will use the results from the CASE2 experiment in our discussions below to provide an estimate of the upper limit of the impact of the stratospheric source.

The annually-averaged, surface NO_y mixing ratio fields from the CASE2 experiments is presented in Figure 8. Lowest surface NO_y mixing ratios are found in the model tropics, while highest levels are found poleward of 60° . The model simulated mixing ratios range from 2-5 pptv in midlatitudes, and from 5-10 pptv in the polar regions. These are extremely low mixing ratios, and are about a factor of 5 to 10 lower than those obtained by Levy *et al.* (1980). Surface NO_y mixing ratios from the CASE2 experiment may also be compared with model calculations of corresponding fields produced by fossil-fuel combustion emissions alone (see Figure 3, Levy and Moxim, 1989). As expected, downward transport from the stratosphere is relatively insignificant over the continental fossil-fuel combustion source regions, and over the Northern Hemisphere midlatitude oceans downwind of these source regions. Our model results also indicate that the stratospheric source may have a greater impact on surface NO_y than the fossil-fuel source in the mid- and high latitude Southern Hemisphere away from fossil-fuel combustion regions.

A more detailed comparison of model calculated, annually-averaged surface mixing ratios with multiple year observations from the SEAREX network (Prospero and Savoie, 1989) is shown in Table 2. While emissions from fossil-fuel combustion explain 40-50% of observed nitrate levels in the North Pacific (assuming most of the model NO_y from the fossil-fuel source is in the form of HNO_3 at these remote locations), transport from the stratosphere usually accounts for less than 2% of observed nitrate at these sites. Discrepancies between model simulations and observations in the tropical South Pacific, where less than 10% of observed nitrate can be accounted for by fossil-fuel combustion and stratospheric injection, suggest an important role for other sources such as biomass burning, NO_x production by lightning discharges, or biogenic emissions associated with soil microbial activity. We once again caution, however, that this conclusion is preliminary, at least in a quantitative sense, since the fossil-fuel simulation has not yet been exercised

with the current chemical and wet removal schemes.

It is also instructive to compare model surface PAN mixing ratios with some recent measurements at high northern latitudes during the ABLE-3A experiment (Singh *et al.*, 1991a). The median PAN level in the 0-2 km altitude range during July was of the order of 25 pptv (see Figure 2, Singh *et al.*, 1991a). Our July-mean PAN mixing ratios from the CASE2 experiment are less than 2 pptv between the surface and the 835 mb model level, between 60° N and 70°N over Alaska. It thus seems unlikely that the stratospheric source is an important factor in determining the tropospheric NO_y budget of this region.

An analysis of deposition fields from the experiment also reveals that stratospheric injection has a negligible impact on observed deposition rates at remote locations, as previously argued by Logan (1983). Observed NO_y deposition rates at these locations range from 2 - 4 mMoles N m⁻² year⁻¹, while deposition rates due to the stratospheric source are generally less than 0.1 mMoles N m⁻² year⁻¹.

4.4 Mid- and upper troposphere mixing ratios

The previous section demonstrated that the stratospheric source appears to have a negligible impact on lower tropospheric NO_y concentrations, both in the remote tropics and at high latitudes. We now turn our attention to the mid- and upper troposphere. Consider the model derived, annually-averaged, 500 mb mixing ratio fields from the CASE2 experiment (Figure 9). This plot may be compared with the corresponding map from Levy and Moxim (1989) for a simulation with the fossil-fuel combustion source alone. In the tropics, the two sources yield comparable NO_y mixing ratios, ranging from 5 to 20 pptv. Mixing ratios from combustion emissions range from 50 pptv to greater than 100 pptv in the northern mid-latitudes, with the larger values occurring at, and downwind of, the major source regions in North America, Europe, and Asia. The corresponding mixing ratios from the CASE2 experiment are of the order of 20-50 pptv south of about 40°N, and 50-100 pptv at higher latitudes. In the Southern Hemisphere mid-troposphere, NO_y mixing-ratios

from the fossil-fuel source range from 10 to 20 pptv near continental source regions, with smaller values (< 5 pptv) occurring in more remote locations. This is because very little NO_y from the Northern Hemisphere combustion emissions is transported to the Southern Hemisphere due to efficient removal at the ITCZ. Model-simulated NO_y mixing ratios from the stratospheric source range from 10-20 pptv in the Southern Hemisphere midlatitudes, and from 20-50 pptv poleward of 60°S, indicating that the stratospheric source is at least as, if not more, important than the fossil-fuel source over much of the Southern Hemisphere mid-troposphere. Higher up in the troposphere, at the 315 mb model level, NO_y mixing ratios from the stratospheric source are about a factor of 2 higher than those produced by the fossil-fuel source during summer in the Northern Hemisphere midlatitudes. However, the stratospheric source dominates during winter/spring in the Northern Hemisphere since this is the period of strongest downward transport from the stratosphere, and also due to the fact that convective upward transport of fossil-fuel NO_y is at a minimum during this period.

The available observational data on total NO_y in the middle and upper troposphere consists of relatively short term measurements, confined to a few specific locations. It is instructive, however, to compare model results with these observations. NO_y measurements over one Southern Hemisphere station (Darwin, Australia; 12° S, 131°E), and two Northern Hemisphere stations (Guam; 14° N, 145°E, and Hickam Air Force Base, Hawaii; 21° N, 158° W) were conducted as part of the Stratosphere-Troposphere Exchange Program (STEP) during January and February, 1987. Our model calculations yield January-average mixing ratios in the range of 10 to 50 pptv in the vicinity of Darwin and Guam at the 190 and 315 mb model levels, while the average observed mixing ratio is approximately 400 pptv (Murphy *et al.*, 1990). Similarly, at Hawaii model calculated values (20-100 pptv) differ substantially from the observations (250-600 pptv). Estimates of NO_y levels from the fossil-fuel combustion source (Levy and Moxim, 1989) are insufficient to account for more than a small fraction of these measurements. This large discrepancy

between observations and model calculations points to an important role for other NO_y sources such as biomass burning and production of NO_x by lightning discharges. While the biomass burning source could account for at least part of the deficit in the northern tropics, it cannot explain the large deficit at the Southern Hemisphere site, especially since the particular time period does not correspond to the burning season in the southern tropics. Taking into account the fact that the measurement period corresponds to the Southern Hemisphere lightning season (Orville and Henderson, 1986), it seems plausible that NO_x production by lightning discharges (as suggested by Murphy *et al.*, 1990) could be the dominant source of NO_y in the southern tropics during this period.

An additional set of NO_y measurements in the middle troposphere are those performed as part of the NASA GTE/CITE II experiment during August and September, 1986, over the eastern North Pacific between 30° and 45°N . Values ranging from ~ 150 pptv to greater than 800 pptv, with a mean of ~ 300 pptv, were observed at altitudes of 4.5-6 km (Ridley *et al.*, 1990). Our model simulations yield mixing ratios ranging from 20 to 50 pptv at the 500 mb model level from the stratospheric source, which leads us to the conclusion that the NO_y mixing ratios over this region of the North Pacific are not strongly influenced by the stratospheric source. Calculations by Levy and Moxim (1989) suggest that export of fossil-fuel combustion emissions from continental source regions results in NO_y mixing ratios ranging from 50 pptv to 200 pptv over this region during the summer. Once again, emissions associated with biomass burning in Asia, and NO_x production by lightning may account for the remaining part of the NO_y . However, the relative importance of these two sources in this region remains to be quantified.

It is also interesting to note that July-mean PAN mixing ratios from the CASE2 simulation range from 10 to 20 pptv between the 315 and 500 mb model levels, over Alaska between 60° and 70°N . These values may be compared with the observed median PAN mixing ratio of ~ 270 pptv during the ABLE-3A experiment (Singh *et al.*, 1991) at an altitude range of 4-6 km, again suggesting that the stratospheric source is a minor contributor to

the tropospheric NO_y budget at high latitudes.

SUMMARY

In this study, we have reevaluated the hypothesis that downward transport of NO_y produced in the stratosphere might explain as much as half the observed surface NO_y in the remote troposphere. Using specified, zonally-averaged O_3 and N_2O fields, along with monthly-averaged pressure and temperature fields from the GFDL 'SKYHI' GCM, we have calculated a temporally varying, two-dimensional NO source function for input into a GCTM. Our model simulations, with a partitioning of NO_y into NO_x , HNO_3 , and PAN, suggest that earlier estimates of surface NO_y concentrations, resulting from downward transport of NO_x produced in the stratosphere, may be overestimated by a factor of 5 to 10. Our current study also indicates that model calculations which do not incorporate PAN chemistry may significantly underpredict NO_x and NO_y concentrations in the lower troposphere. A more realistic treatment of the chemistry of long-lived organics in global transport models is clearly an area which warrants further investigation, as it could have major implications for our understanding of NO_y distributions from other sources as well.

The model results, in conjunction with an earlier assessment of NO_y distributions from fossil-fuel combustion emissions, imply a major role for other possible sources of surface NO_y in the remote tropics and in the Southern Hemisphere. Comparisons of model calculated mid-tropospheric background NO_y mixing ratios with observations in the tropics and sub-tropics also suggest that biomass burning and nitrogen fixation associated with lightning discharges may contribute significantly to the tropospheric NO_y budget. Uncertainties associated with source strengths, transport, chemistry, and removal still persist. However, we feel that our two principal conclusions regarding the minimal impact of the stratospheric source on remote lower tropospheric NO_y mixing ratios, and the need for a significant source of NO_y in the tropical mid- and upper troposphere, are valid.

ACKNOWLEDGEMENTS

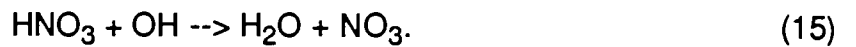
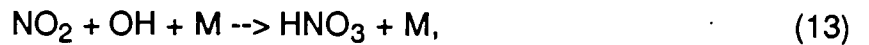
This work was supported in part by funds from the National Science Foundation under grant ATM-8701289. We wish to thank D. W. Fahey, K. Hamilton, J. D. Mahlman, D. M. Murphy, and S. E. Strahan for their perceptive comments on the original manuscript. We are especially grateful to S. C. Liu and an anonymous reviewer for their thoughtful comments and suggestions. We also wish to express our gratitude to D. M. Murphy and D. W. Fahey for providing unpublished data.

APPENDIX

PARTITIONING OF NO_y INTO SOLUBLE AND INSOLUBLE SPECIES

An accurate determination of the fraction of the individual nitrogen species that make up NO_y requires the solution of a coupled set of stiff partial differential equations. Since solution methods for these types of systems are extremely time consuming, various simplifying assumptions are often made to obtain approximate solutions to this problem. We describe below a simplified chemical scheme, which enables us to explicitly calculate the partitioning of NO_y into soluble and insoluble fractions, without resorting to iterative solution schemes. Chemical production and loss rates of the soluble and insoluble fractions are calculated based on the reaction of NO₂ and HNO₃ with OH, and the photodissociation of HNO₃. The essence of the method involves capturing the spatial variation of the OH concentration field, and scaling these concentrations so as to yield a tropospheric methyl chloroform lifetime of 6.2 years (Prinn *et al.*, 1987). The set of chemical reactions considered are:





Using recent estimates of kinetic parameters (DeMore *et al.*, 1990), specified one-dimensional NO_x and CO profiles in each hemisphere (Figure 10), specified two-dimensional O_3 (see Figure 1) and CH_4 fields (Figure 11), and monthly average temperature, pressure, and water vapor fields from the GFDL 'SKYHI' GCM (Hamilton and Mahlman, 1988), from (1) and (2) we calculate zonally averaged $\text{O}(^1\text{D})$ concentrations as

$$n(O^1D) = \frac{J_1 n(O_3)}{k_2 n(M)}, \quad (A1)$$

where, the n 's represent number densities, J_i is the photolysis rate coefficient for reaction i , and k_j is the specific reaction rate for reaction j . The NO/NO_2 ratio is calculated from (11) and (12) based on the assumption of a photostationary state between NO , NO_2 , and

O₃ as

$$\frac{n(NO)}{n(NO_2)} = \frac{J_{11}}{k_{12} n(O_3)}, \quad (A2)$$

and NO and NO₂ concentrations are calculated using the specified NO_x concentrations.

From reactions (6) - (10), and assuming that the HO₂ - OH cycling reactions are relatively rapid enables us to write

$$RATIO = \frac{n(HO_2)}{n(OH)} = \frac{k_6 n(CH_4) + k_7 n(CO) + k_8 n(O_3)}{k_9 n(O_3) + k_{10} n(NO)}. \quad (A3)$$

Based on a balance between radical production and destruction (reactions (3), (4a), (4b), (5a), and (5b)), and using the HO₂/OH ratio calculated from (A3), we calculate the OH concentration as

$$n(OH) = \left[\frac{k_3 n(O^1D) n(H_2O)}{k_4 (RATIO) + k_5 (RATIO)^2} \right]^{\frac{1}{2}} \times FACT, \quad (A4)$$

where, *FACT* is an empirically determined correction factor. This correction factor is determined by scaling the OH fields to yield a globally and annually averaged methyl chloroform lifetime of 6.2 years (Prinn *et al.*, 1987). Specifically, we obtain *FACT* ≈ 2, and a scaled globally and annually averaged tropospheric OH concentration of 6.7 × 10⁵ molecules cm⁻³. The large value of the correction factor is due to the simplifying assumptions made to facilitate the OH calculation. The zonally averaged, scaled tropospheric OH fields calculated in this manner compare reasonably well with tropospheric OH fields derived using a more detailed implicit chemical scheme based on a CH₄-CO-NO_x-O₃-H_xO_y mechanism (e.g., Chameides and Tan, 1981; Spivakovsky *et al.*, 1990). The sharp gradients in the boundary layer near the equator are related to the very simple, hemispherically averaged, one-dimensional distribution assumed for NO_y.

We then use these scaled OH fields to specify NO_x/HNO₃ production and destruction rates in the form of 'look-up' tables to the transport model. While the simple chemical

scheme clearly has limitations, especially in its treatment of the radical cycling reactions, these are not of great significance in this study since a large fraction of the NO_y transported to the troposphere from the stratosphere is in the form of HNO₃, and this feature is captured with the simple chemical scheme.

REFERENCES

- Atkinson, R., and Lloyd A. C., Evaluation of kinetic and mechanistic data for modeling of photochemical smog, *J. Phys. Chem. Ref. Data*, **13**, 315 - 440, 1984.
- Cadle, S. H., Dasch, J. M., and Mulawa, P. A., Atmospheric concentrations and the deposition velocity to snow of nitric acid, sulfur dioxide and various particulate species, *Atmos. Environ.*, **19**, 1819 - 1827, 1985.
- Chameides W. L., and Tan, A., The two-dimensional diagnostic model for tropospheric OH : An uncertainty analysis, *J. Geophys. Res.*, **86**, 5209 - 5223, 1981.
- Crutzen, P. J., Photochemical reaction initiated by and influencing ozone in unpolluted tropospheric air, *Tellus*, **26**, 45 - 55, 1974.
- Crutzen, P. J., and Schmailzl, U., Chemical budgets of the stratosphere, *Planet. Space Sci.*, **31**, 1009 - 1020, 1983.
- DeMore, W. B., Margitan, J. J., Molina, M. J., Watson, R. T., Golden, D. M., Hampson, R. F., Kurylo, M. J., Howard, C. J., and Ravishankara, A. R., *Chemical kinetics and photochemical data for use in stratospheric modeling, Evaluation number 9*, NASA, JPL Publication 90-1, Jet Propulsion Laboratory, Pasadena, California, 217 pp, 1990.
- Giorgi, F., and Chameides, W. L., Rainout lifetimes of highly soluble aerosols and gases as inferred from simulations with a general circulation model, *J. Geophys. Res.*, **91**, 14367 - 14376, 1986.
- Hamilton K., and Mahlman, J. D., General circulation model simulation of the semiannual oscillation of the tropical middle atmosphere, *J. Atmos. Sci.*, **45**, 3214 - 3235, 1988.
- Huebert, B. J., Nitric acid and aerosol nitrate measurements in the equatorial Pacific region, *Geophys. Res. Lett.*, **7**, 325 - 328, 1980.
- Huebert, B. J., and Robert, C. H., The dry deposition of nitric acid to grass, *J. Geophys. Res.*, **90**, 2085 - 2090, 1985.

- Jackman, C. H., Frederick, J. E., and Stolarski, R. S., Production of odd nitrogen in the stratosphere and mesosphere: An intercomparison of source strengths, *J. Geophys. Res.*, **85**, 7495 - 7505, 1980.
- Kley, D., Drummond, J. W., McFarland, M., and Liu, S. C., Tropospheric profiles of NO_x, *J. Geophys. Res.*, **86**, 3153- 3161, 1981.
- Legrand, M. R., Stordal, F., Isaksen, I. S. A., and Rognerud, B., A model study of the stratospheric budget of odd nitrogen including effects of solar cycle variations, *Tellus*, **41**, 413 - 426, 1989.
- Leighton, P. A., *Photochemistry of air pollution*, Academic Press, New York, 300 pp., 1961.
- Levy II, H., Normal atmosphere: Large radical and formaldehyde concentrations predicted, *Science*, **173**, 141 - 143, 1971.
- Levy II, H., Mahlman, J. D., and Moxim, W. J., A stratospheric source of reactive nitrogen in the unpolluted troposphere, *Geophys. Res. Lett.*, **7**, 441 - 444, 1980.
- Levy II, H., Mahlman, J. D., and Moxim, W. J., Tropospheric N₂O variability, *J. Geophys. Res.*, **87**, 3061 - 3080, 1982.
- Levy II, H., Mahlman, J. D., Moxim, W. J., and Liu, S. C., Tropospheric ozone: The role of transport, *J. Geophys. Res.*, **90**, 3753 - 3772, 1985.
- Levy II, H., and Moxim, W. J., Simulated global distribution and deposition of reactive nitrogen emitted by fossil fuel combustion, *Tellus*, **41**, 256 - 271, 1989.
- Liu, S. C., Kley, D., McFarland, M., Mahlman, J. D., and Levy II, H., On the origin of tropospheric ozone, *J. Geophys. Res.*, **85**, 7546 - 7552, 1980.
- Logan, J. A., Nitrogen oxides in the troposphere: Global and regional budgets, *J. Geophys. Res.*, **88**, 10785 - 10807, 1983.
- Madronich, S., and Calvert J. G., Permutation reactions of organic peroxy radicals in the troposphere, *J. Geophys. Res.*, **95**, 5697 - 5716, 1990.
- Mahlman, J. D., and Moxim, W. J., Tracer simulation using a global general circulation model: Results from a midlatitude instantaneous source experiment, *J. Atmos. Sci.*, **35**, 1340 - 1374, 1978.
- Mahlman, J. D., Levy II, H., and Moxim, W. J., Three-dimensional tracer structure and behavior as simulated in two ozone precursor experiments, *J. Atmos. Sci.*, **37**, 655 - 685, 1980.
- Mahlman, J. D., Levy II, H., and Moxim, W. J., Three-dimensional simulations of strato-

- spheric N₂O: Predictions for other trace constituents, *J. Geophys. Res.*, *91*, 2687 - 2707, 1986.
- Manabe, S., Hahn, D. G., and Holloway, Jr., J. L., The seasonal variation of the tropical circulation as simulated by a global model of the atmosphere, *J. Atmos. Sci.*, *31*, 43 - 83, 1974.
- Manabe, S., and Holloway, Jr., J. L., The seasonal variation of the hydrologic cycle as simulated by a global model of the atmosphere, *J. Geophys. Res.*, *80*, 1617 - 1649, 1975.
- Manabe, S., and Mahlman, J. D., Simulation of seasonal and interhemispheric variations in the stratospheric circulation, *J. Atmos. Sci.*, *33*, 2185 - 2217, 1977.
- Murphy, D. M., Fahey, D. W., Liu, S. C., Proffitt, M. H., and Eubank, C. S., Measurements of reactive odd nitrogen and ozone in the upper troposphere and lower stratosphere, *in preparation*, 1990.
- National Research Council, *Acid deposition: Atmospheric processes in Eastern North America, a review of current scientific understanding*, National Academy Press, Washington, D. C., 375 pp., 1983.
- Oltmans, S. J., Surface ozone measurements in clean air, *J. Geophys. Res.*, *86*, 1174 - 1180, 1981.
- Orville, R. E., and Henderson R. W., Global distribution of midnight lightning: September 1977 to August 1978, *Mon. Wea. Rev.*, *114*, 2640 - 2653, 1986.
- Prinn, R., Cunnold, D., Rasmussen, R., Simmonds, P., Alyea, F., Crawford, A., Fraser, P., and Rosen, P., Atmospheric trends in methylchloroform and the global average for the hydroxyl radical, *Science*, *238*, 945 - 950, 1987.
- Prospero, J. M., and Savoie, D. L., Effect of continental sources on nitrate concentrations over the Pacific Ocean, *Nature*, *339*, 687 - 689, 1989.
- Ridley, B.A., Shetter, J. D., Gandrud, B. W., Salas, L. J., Singh, H. B., Carroll, M. A., Hubler, G., Albritton, D. L., Hastie, D. R., Schiff, H. I., Mackay, G. I., Karechi, D. R., Davis, D. D., Bradshaw, J. D., Rodgers, M. O., Sandholm, S. T., Torres, A. L., Condon, E. P., Gregory, G. L., and Beck, S. M., Ratios of peroxyacetylnitrate to active nitrogen observed during flights over the eastern Pacific oceans and continental United States, *J. Geophys. Res.*, *95*, 10179 - 10192, 1990.
- Rudolph, J., Two-dimensional distribution of light hydrocarbons: Results from the STRATOZ III experiment, *J. Geophys. Res.*, *93*, 8367 - 8377, 1988.
- Rudolph, J., and Muller, K. P., The latitudinal distribution of peroxyacetylnitrate (PAN) in the atmospheric boundary layer over the Atlantic, *Presented at the 7th International*

Symposium of the Commission on Atmospheric Chemistry and Global Pollution, Chamrousse, France, 1990.

Ryther, J. H., and Dunstan, W. M., Nitrogen, phosphorus, and eutrophication in the coastal marine environment, *Science*, 171, 1008 - 1113, 1971.

Savoie, D. L., Prospero, J. M., Merrill, J. T., and Uematsu, M., Nitrate in the Atmospheric boundary layer of the tropical South Pacific: Implications regarding sources and transport, *J. Atmos. Chem.*, 8, 391 - 415, 1989.

Singh, H. B., and Zimmerman, P. B., Atmospheric distributions and sources of non-methane hydrocarbons, *Adv. Env. Sci. Tech.*, submitted, 1990.

Singh, H. B., O'Hara, D., Herlth, D., Bradshaw, J. D., Sandholm, S. T., Gregory, G. L., Sachse, G. W., Blake, D. R., Crutzen, P. J., and Kanakidou, M. A., Atmospheric measurements of PAN and other organic nitrates at high latitudes: Possible sources and sinks, *J. Geophys. Res.*, submitted, 1991a.

Singh, H. B., Herlth, D., O'Hara, D., Zahnle, K., Bradshaw, J. D., Sandholm, S. T., Talbot, R., Crutzen, P. J., and Kanakidou, M. A., Relationship of PAN to active and total odd nitrogen at northern high latitudes: Influence of reservoir species on NO_x and O₃, *J. Geophys. Res.*, submitted, 1991b.

Spivakovsky, C. M., Yevich, R., Logan, J. A., Wofsy, S. C., McElroy, M. B., and Prather, M. J., Tropospheric OH in a three-dimensional chemical tracer model: An assessment based on observations of CH₃CCl₃, *J. Geophys. Res.*, 95, 18441 - 18472, 1990.

Voldner, E. C., Barrie, L. A., and Sirois, A., A literature review of dry deposition of oxides of sulfur and nitrogen with emphasis on long-range transport modeling in North America, *Atmos. Environ.*, 20, 2101 - 2123, 1986.

Walcek, C. J., Brost, R. A., Chang, J. S., and Wesely, M. L., SO₂, sulfate, and HNO₃ deposition velocities computed using regional land use and meteorological data, *Atmos. Environ.*, 20, 949 - 964, 1986.

Wesely, M. L., Eastman, J. A., Stedman, D. H., and Yalvac, E. D., An eddy correlation measurement of NO₂, *Atmos. Environ.*, 16, 815 - 820, 1982.

World Meteorological Organization, *Atmospheric ozone 1985, WMO Global Ozone Research and Monitoring Project, Report No. 16*, 648 pp., Geneva, 1985.

TABLE 1

COMPARISON OF MODEL RESULTS WITH LIMS DERIVED LOWER STRATOSPHERIC NO_y FOR JANUARY¹

<u>LOCATION</u>	<u>OBSERVATIONS²</u>	<u>MODEL³</u>
64°S	9 - 10	5 - 6
48°S	~8	~5
32°S	~6	3 - 4
16°S	~2	1 - 2
Equator	<2	~2
16°N	~3	4 - 5
32°N	~9	6 - 7
48°N	~13	10 - 11

-
1. Observations are for January, 1979, at approximately 50 mb (see Figure 10-68, World Meteorological Organization (1985)).
 2. LIMS derived NO_y in ppbv.
 3. Monthly average NO_y (ppbv) from the CASE1 simulation obtained by interpolating data from 38 and 65 mb model levels.

TABLE 2COMPARISON OF CASE2 MODEL RESULTS WITH SEAREX SURFACE OBSERVATIONS¹

<u>STATION</u>	<u>OBS</u> ²	<u>COMB</u> ³	<u>STRAT</u> ⁴			
			<u>NO_x</u>	<u>HNO₃</u>	<u>PAN</u>	<u>NO_y</u>
Shemya (53°N, 174°E)	94	74	2	<1	3	5
Midway (28°N, 177°W)	104	62	1	1	<1	3
Oahu (21°N, 158°W)	130	49	1	1	<1	2
Enewetak (11°N, 162°E)	56	25	<1	1	<1	1
Fanning (4°N, 159°W)	59	16	<1	<1	<1	<1
Nauru (1°S, 167°E)	59	7	<1	<1	<1	<1
Funafuti (8°S, 179°E)	39	6	<1	<1	<1	1
Samoa (14°S, 171°W)	40	6	<1	<1	<1	1
Rarotonga (21°S, 160°W)	42	6	<1	<1	<1	1
New Caledonia (22°S, 166°E)	76	55	1	1	<	2
Norfolk Island (29°S, 169°E)	66	30	1	1	<1	2

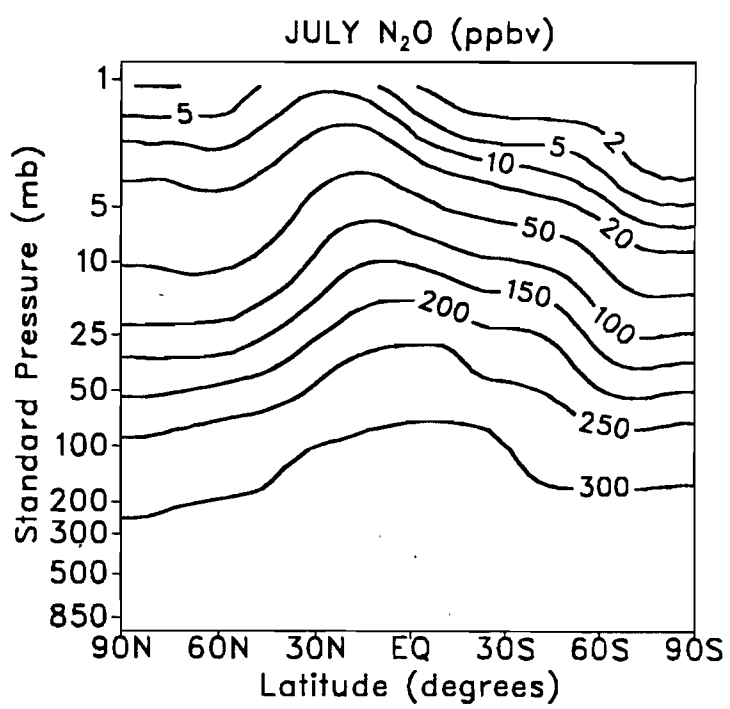
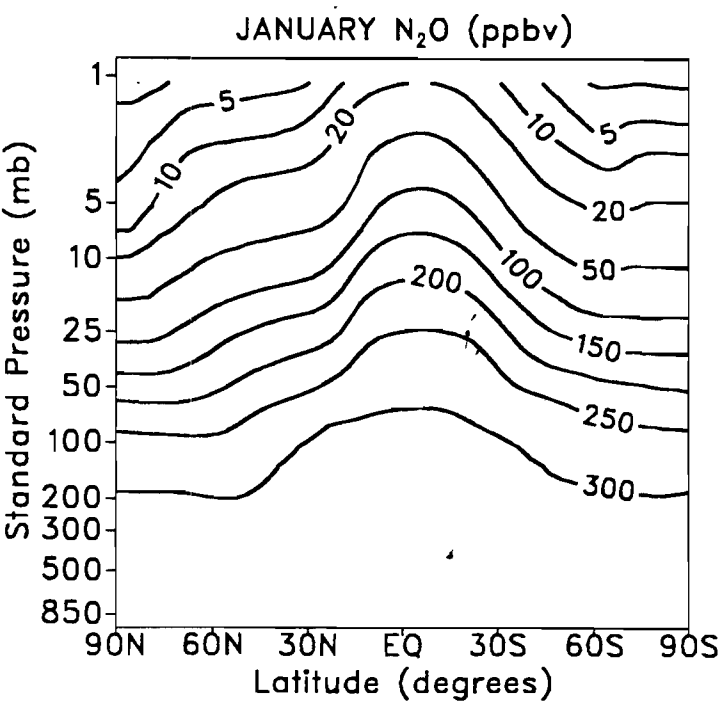
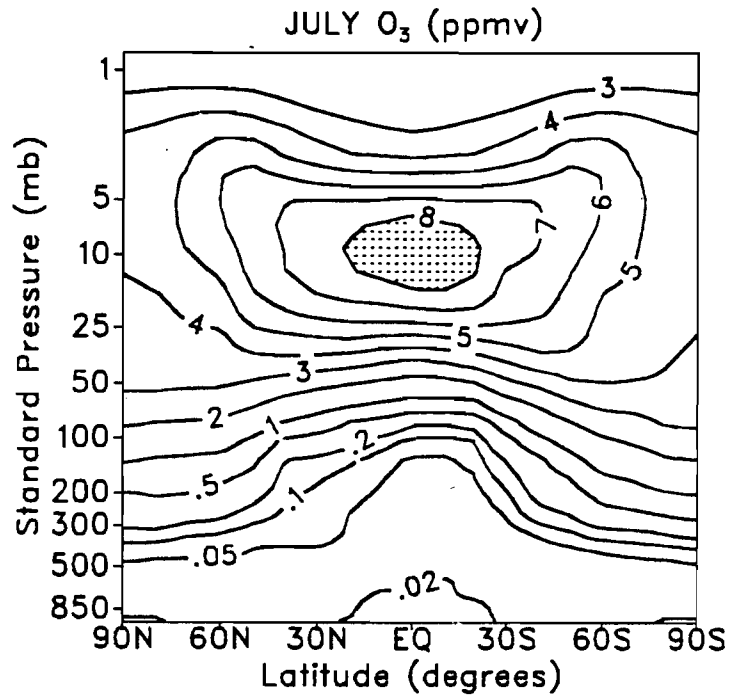
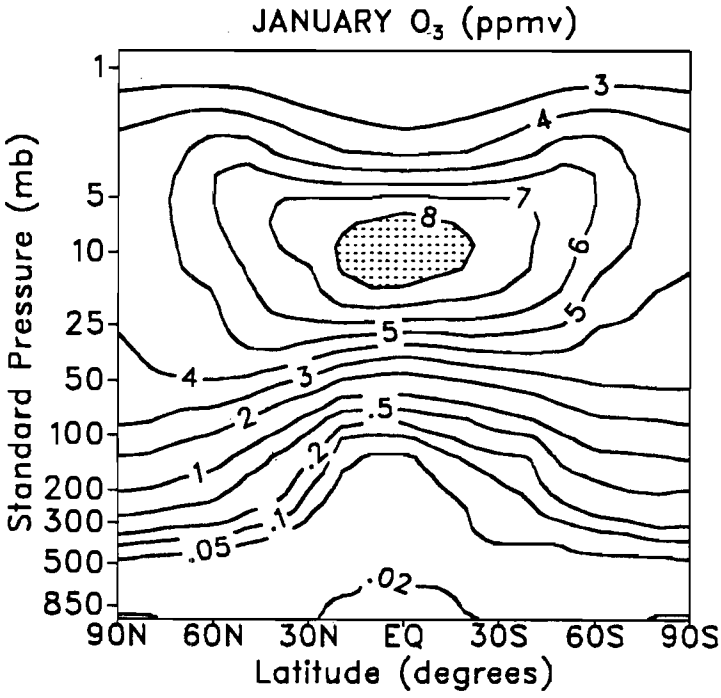
-
1. Observations are soluble reactive nitrogen measurements, while model results are at the 990 mb model level. All values are in pptv.
 2. Soluble reactive nitrogen measurements from Prospero and Savoie (1989).
 3. Model NO_y with the fossil-fuel combustion source alone from Levy and Moxim (1989).
 4. Model results from the CASE2 experiment.

FIGURE CAPTIONS

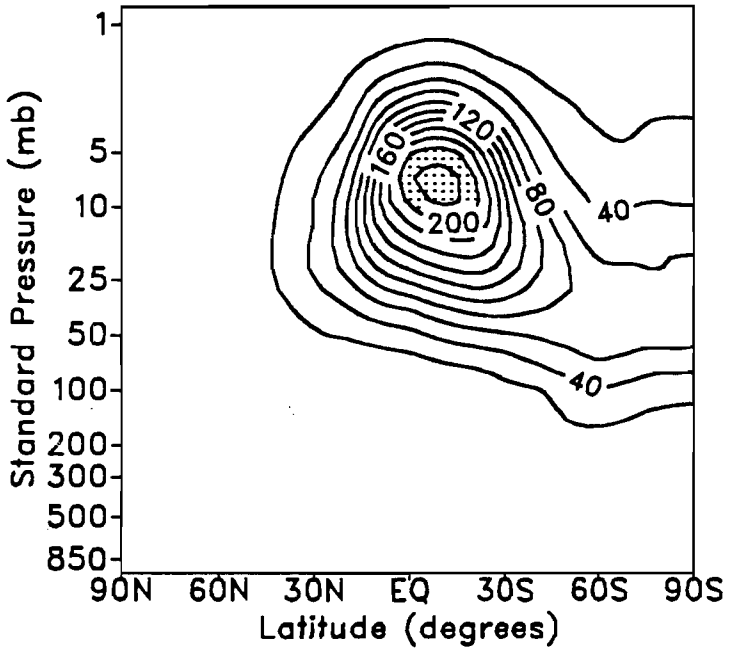
1. Monthly-average O_3 (ppmv) and N_2O (ppbv) fields used in the calculation of the stratospheric NO_x source. Contour levels for O_3 are 0.02, 0.05, 0.1, 0.2, 0.5, 1, 2, 3, 4, 5, 6, 7, and 8 ppmv. Contour levels for N_2O are 2, 5, 10, 20, 50, 100, 150, 200, 250, and 300 ppbv.
2. Calculated NO production rates ($\text{molecules cm}^{-3} \text{ s}^{-1}$) for indicated months. Contour levels range from 20 to 220, in increments of 20.
3. Monthly-average, zonal-mean NO_y mixing ratios (ppbv) for indicated months from the CASE1 experiment. Contour levels are logarithmic.
4. Monthly-average, zonal-mean mixing ratios (ppbv) of a) NO_x and b) HNO_3 from the CASE1 experiment for the indicated months. Contour levels are logarithmic.
5. Ratio of model calculated NO_y mixing ratios with PAN chemistry (CASE2 experiment) to mixing ratios obtained without including PAN chemistry (CASE1 experiment). Lightly shaded areas represent regions where CASE2 results are less than or equal to CASE1 results, while heavily shaded areas represent regions where CASE2 results are at least a factor of 2 higher than CASE1 results. Contour levels are 1, 1.1, 1.3, 1.5, 2, 3, and 4.
6. Ratio of model calculated NO_x and HNO_3 mixing ratios from CASE2 experiment to mixing ratios from the CASE1 experiment. Lightly shaded areas represent regions where CASE2 results are less than or equal to CASE1 results, while heavily shaded areas represent regions where CASE2 results are at least a factor of 2 higher than CASE1 results. Contour levels are 0.8, 0.9, 1, 1.1, 1.3, 1.5, 2, 3, 4, and 5.
7. Monthly-average, zonal-mean PAN mixing ratios from the CASE2 experiment for the indicated months. Contour levels are logarithmic.
8. Annually-averaged surface NO_y mixing ratios (pptv) CASE2 experiment. Contour levels are logarithmic
9. Annually-averaged 500 mb NO_y mixing ratios (pptv) from the CASE2 experiment. Con-

four levels are logarithmic

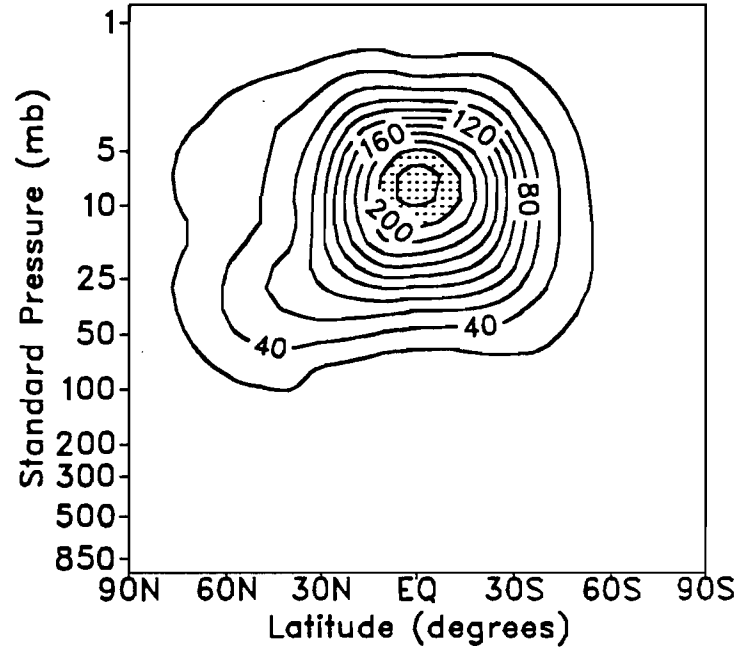
10. Prescribed one-dimensional NO_x (light lines) and CO (heavy lines) vertical profiles used in the calculation of tropospheric OH fields. Solid lines represent Northern Hemisphere profiles, while dashed lines represent Southern Hemisphere profiles.
11. Prescribed CH_4 field (ppmv) used in the calculation of tropospheric OH fields. Contour levels are 0.2, 0.4, 0.6, 0.8, 1.0, 1.2, 1.4, 1.6, 1.65, 1.7, and 1.75 ppmv.



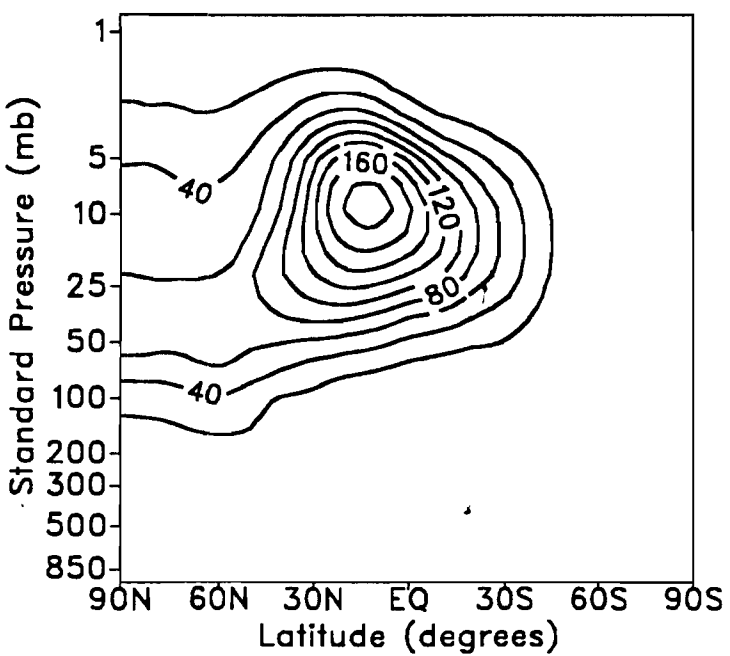
JANUARY



APRIL



JULY



OCTOBER

